

Evidence for Universality of Near Infrared Color Evolution of Type Ia Supernovae, and Implications for Host Galaxy Extinction Determination ¹

Kevin Krisciunas², Alan Diercks³, N. C. Hastings², Karen Loomis⁴, Eugene Magnier⁵,
Russet McMillan⁴, Adam G. Riess⁶, and Christopher Stubbs²

²Department of Astronomy, University of Washington, Box 351580, Seattle, WA
98195–1580

³Department of Astronomy, California Institute of Technology, Mail Code 105-24,
Pasadena, CA 91125

⁴Apache Point Observatory, Astrophysical Research Consortium, 2001 Apache Point Road,
P. O. Box 59, Sunspot, NM 88349-0059

⁵Canada-France-Hawaii Telescope Corporation, PO Box 1597, Kamuela, HI 96743

⁶Space Telescope Science Institute, 3700 San Martin Drive, Baltimore, MD 21218

Electronic mail: kevin, hastings, stubbs@astro.washington.edu

ad@astro.caltech.edu

eugene@cfht.hawaii.edu

karen, rmcmillan@apo.nmsu.edu

ariess@stsci.edu

Received _____; accepted _____

¹Based on observations obtained with the Apache Point Observatory 3.5-meter telescope, which is owned and operated by the Astrophysical Research Consortium.

ABSTRACT

From an analysis of SNe 1972E, 1980N, 1981B, 1981D, 1983R, and 1999cp we find that the intrinsic $V-K$ colors of Type Ia SNe with multi-color light curve shape (MLCS) parameter $-0.38 \leq \Delta \leq +0.20$ exhibit a universal color curve. $V-K$ colors become bluer linearly with time from 9 days before B-band maximum until 6 days after maximum, after which they redden linearly until 27 days after maximum. $V-H$ colors exhibit very similar color evolution. $V-J$ colors exhibit slightly more complex evolution, with greater scatter. The existence of V *minus* near infrared color relations allows the construction of near infrared light curve templates that are an improvement on those of Elias et al. (1985).

We provide optical BVRI and infrared JHK photometry of the Type Ia supernovae 1999aa, 1999cl, and 1999cp. SN 1999aa is an overluminous “slow decliner” (with $\Delta = -0.47$). SN 1999cl is extremely reddened in its host galaxy, with $E(B-V) \approx 1.14$; this reddening is most likely local to its environment and is anomalous compared to Galactic reddening. SN 1999cp is a moderately bright SN unreddened in its host.

A comparison of V *minus* near infrared colors of unreddened SNe with the moderately reddened SN 1998bu gives $A_V = 1.14 \pm 0.07$ for this object, in excellent agreement with the results based solely on optical photometry. For SN 1999cl prior to 7 days after B-band maximum the V *minus* near infrared colors yield $A_V = 1.83 \pm 0.20$. This leads to a distance for its host galaxy (M 88) in agreement with other distance measurements for members of the Virgo cluster.

Subject headings: supernovae, photometry

1. Introduction

In order to obtain the distance d (in pc) to a celestial object from its brightness we must know three things: (1) an accurate apparent magnitude m of the object; (2) an estimate of the object's absolute magnitude M ; and (3) an estimate of any extinction along the line of sight. These four parameters are related by the standard equation:

$$M_\lambda = m_\lambda - A_\lambda + 5 - 5 \log d, \quad (1)$$

where A_λ is the extinction in magnitudes. Extinction is a serious source of systematic errors in determining distances. Each 0.1 mag error due to extinction, absolute magnitude, or apparent magnitude corresponds to a 5 percent error in the distance to the object. The primary focus of this paper is to outline a method of determining the V-band extinction, A_V , towards Type Ia supernovae. For a discussion of the absolute magnitudes see Meikle (1999).

1.1. Apparent magnitudes

At present more than 100 supernovae (SNe, singular SN) are discovered each year.⁷ In many cases a low redshift SN appears at a substantial angular distance from the galaxy or appears on a rather uniform swath of galaxy light. In these cases aperture photometry will give an accurate apparent magnitude for the supernova without having to worry about contamination by other sources of photons. One can further justify the use of aperture photometry of a visible SN by obtaining a Digital Sky Survey image of its host galaxy,

⁷As of December 1, 1999 there have been 188 SNe discovered this year, given the naming scheme of the IAU Circulars. In 1998 the total was 160.

displaying it with IRAF and using the **imexam** package to gauge how problematic the location of the SN is.

In many other cases, however, the supernova is superimposed on an arm or the core of a galaxy, or it could be a small angular distance from a bright foreground star in our Galaxy, so the best way to obtain the apparent magnitude of the SN by itself is to subtract a template image of the sky-without-supernova from the images of the sky-with-supernova. However, one usually does not have appropriately exposed images in all relevant filters of such a field before the SN has appeared. Thus, one must wait a year or longer to obtain the galaxy template images.

1.2. Absolute magnitudes

In order to know the absolute magnitudes of Type Ia SNe we need to observe a number of extinction corrected Type Ia SNe in galaxies with known distances. Observations of Type Ia supernovae over the past decade have shown that while Type Ia SNe are not standard candles *per se*, they are standardizable candles, forming a single-parameter family.

Phillips (1993) and Hamuy et al. (1996) noted a relationship between the rate of decline of Type Ia SNe and their intrinsic luminosities, characterized by the number of magnitudes these objects decline in the first 15 days after B-band maximum. The Phillips relation shows that Type Ia SNe with smaller values of $\Delta m_{15}(B)$ are intrinsically more luminous. A typical value of $\Delta m_{15}(B)$ is 1.1.

Riess, Press & Kirshner (1996a, hereafter RPK) and Riess et al. (1998) outlined the multi-color light curve shape (MLCS) method of fitting Type Ia SN photometry. The key parameter, which they call Δ , is basically the number of magnitudes that a Type Ia SN is brighter than or fainter than some fiducial object. In other words, $\Delta \equiv M_V -$

M_V (fiducial). Objects with $\Delta < 0$ are more luminous and decline more slowly after maximum light; objects with $\Delta > 0$ are less luminous and more rapidly declining.⁸ Using Cepheid calibrations of a set of nearby SNe, Jha et al. (1999b) find $M_V = -19.34$ for the fiducial Type Ia SN with $\Delta = 0.0$. The MLCS method uses the data for four photometric bands (BVRI) and simultaneously gives the light curve solutions, the reddening along the line of sight to the SN (i.e. the *sum* of the reddening in our Galaxy and the reddening within the host galaxy), the time of maximum light,⁹ and the distance modulus of the SN.

A third method for characterizing the light curves of Type Ia SNe is the “stretch factor” method of Perlmutter et al. (1997). The stretch factor is used to broaden or narrow the rest-frame timescale of a template light curve. The Phillips parameter ($\Delta m_{15}(B)$) and the stretch factor (s) are related (Perlmutter et al.) as follows:

$$\Delta m_{15}(B) = 1.96 \pm 0.17(s^{-1} - 1) + 1.07. \quad (2)$$

All three empirical fitting methods are attempts to model the differences in light curve shape, attributable to a range of absolute magnitudes, which in turn are attributable to the details of the explosions giving rise to the various Type Ia SNe (Höflich & Khokhlov 1996; Nomoto, Iwamoto & Kishimoto 1997).

⁸We make reference in this paper to “slow decliners” and “fast decliners” and hope that no confusion arises as a result; in fact, there is a continuum of decline rates.

⁹Throughout this paper we shall define the time of maximum to be the B-band maximum; V-band maximum occurs about 2 days after B-band maximum. Time t will be the number of days since B-band maximum.

1.3. Interstellar reddening and absorption

If we have a sample of nearby Type Ia SNe which occurred at a significant angular distance from any spiral arms or the central bulges of the host galaxies, we might safely assume they were unreddened in their hosts, and that their B–V colors are intrinsic to these objects. Schaefer (1995) noted that Type Ia SNe with “normal” spectra and/or decline rates have an intrinsic $B-V = 0.00 \pm 0.04$ at light maximum. This would imply that if a Type Ia SN has an *observed* $B-V$ color at light maximum of, say, 0.20, then its color excess $E(B-V) \equiv A_B - A_V \approx 0.20$. Using the standard value of $R_V \equiv A_V / E(B-V) = 3.1$ (Sneden et al. 1978, Rieke & Lebofsky 1985), and assuming that dust in the host galaxy of a SN is the same as dust in our Galaxy (Riess, Press, & Kirschner 1996b), we can determine the V-band extinction to the object. With an estimate of the SN’s absolute magnitude from any of the three light curve fitting methods described above we can then determine the distance to the SN and its host galaxy.

RPK had as one of their motivations for MLCS that there was nearly a one magnitude range of intrinsic color at light maximum for Type Ia SNe. Assuming that all Type Ia SNe have the same color at maximum actually increases the scatter of the Hubble diagram. For example, observations of SN 1991bg (Leibundgut et al. 1993) and our own observations of SN 1999da (Krisciunas et al. 1999) show that these two “fast decliners” had $B-V \approx 0.74$ at the time of light maximum. “Slow decliners” such as SN 1991T (Lira et al. 1998) can have excess short wavelength (U-band and B-band) light. The MLCS method takes into account these differences in color to some extent, but we must remind the reader that MLCS is still based on a relatively small number of objects. Just because a SN’s photometry does not fit MLCS templates does not mean that the photometry is wrong.

Lira (1995) and Phillips et al. (1999, in particular, their Fig. 1) have shown that *all* unreddened Type Ia SNe, no matter what their decline rates, have essentially the same

B–V color evolution from 30 to 90 days after V-band maximum. (This is also shown graphically by RPK.) They find

$$(B - V)_0 = 0.725 - 0.0118 (t_V - 60) . \quad (3)$$

If Eq. 3 holds for all Type Ia SNe, then we may use it and accurate measurements of the observed B–V color between 30 and 90 days after V-band maximum to determine $E(B - V)$. The primary drawback of Lira’s relation is that by the time a typical SN is one to three months past maximum its V-band light has dimmed by 1.5 to 3 magnitudes and its B-band light has diminished 2.5 to 4 magnitudes.

If we attempt to determine A_V solely from B-band and V-band photometry, any errors in the adopted color excess $E(B - V)$ are scaled by $R_V \approx 3.1$. More specifically, since $A_V = R_V \times E(B - V)$, the uncertainty in A_V will be given by:

$$\sigma_{A_V}^2 = (R_V)^2 \sigma_{E(B-V)}^2 + (E(B - V))^2 \sigma_{R_V}^2 . \quad (4)$$

Given the infrared selective extinction coefficients determined by Rieke & Lebofsky (1985) we use the following relationships between color excess and A_V :

$$A_J = 0.282 A_V \longrightarrow A_V = 1.393 E(V - J) . \quad (5)$$

$$A_H = 0.175 A_V \longrightarrow A_V = 1.212 E(V - H) . \quad (6)$$

$$A_K = 0.112 A_V \longrightarrow A_V = 1.126 E(V - K) . \quad (7)$$

Fig. 1 shows graphically the advantage of determining A_V from a combination of optical and infrared data. Consider the *worst* case scenario, that the coefficient on the left hand part of Eq. 7 is only known to ± 50 percent. Then $A_V = 1.126 \pm 0.072 \times E(V-K)$. For the case of $A_V = 1.00$ mag, $E(V-K) = 0.888$ (solid line in Fig. 1). The dashed line in Fig. 1 is the *best* case scenario for optical data; it assumes $R_V = 3.1 \pm 0.1$ and $E(B-V) = 0.323$ to give $A_V = 1.00$. We know that R_V is not a univeral constant (Cardelli, Clayton, & Mathis 1989). Riess, Press, & Kirshner (1996b) find that the most appropriate value to use for Type Ia SNe is $R_V = 2.55 \pm 0.3$. In Fig. 1 the dotted line uses $R_V = 2.55$ and $E(V-K) = 0.392$ to give $A_V = 1.00$. We claim below that the color excess $E(V-K)$ for Type Ia SNe can be determined to ± 0.1 mag *or better*. While one can determine the $B-V$ color of a supernova to ± 0.02 mag, determining the color *excess* is another matter.

In this paper we shall show that V-band and infrared photometry (at J (1.2 μ m), H (1.65 μ m), and K (2.2 μ m)) can give us a good handle on A_V without scaling up any errors by a factor as large as R_V .

1.4. What data are available?

Very little infrared photometry has been published on Type Ia SNe. The canonical papers are by Elias et al. (1981, 1985). In their second paper (see their Fig. 7) these authors even note the small scatter (± 0.1 mag) in $V-K$ for four Type Ia SNe. Frogel et al. (1987) present much infrared data for the SN 1986G, which was a highly reddened ($E(B-V) \geq 0.6$) “atypical subluminous event” (Phillips et al. 1987, Meikle 1999).

Suntzeff et al. (1999) and Jha et al. (1999b) give optical data for SN 1998bu. Mayya, Puerari, & Kuhn (1998) and Jha et al. (1998b) give infrared data. Meikle & Hernandez (1999) show other infrared data in graphical form, while their data values are found in

Meikle (1999) and will be discussed in full by Hernandez et al. (2000). The photometry of SN 1998bu comprises the first large infrared data set for a “normal” Type Ia SN before maximum. We note that the infrared data of Jha et al. (1999b) prior to B-band maximum are systematically fainter than the infrared data of Mayya et al. (1998) and Meikle (1999), by 0.1 mag or more. We do not address the issue of whose data might be systematically “in error” prior to light maximum. Perhaps the true uncertainties of their data are larger than the errors quoted.

Here we present optical BVRI and infrared JHK data on SNe 1999aa, 1999cl, 1999cp, including infrared data on two of the three before maximum.

We shall show that $V-K$ colors are much more useful for investigating Type Ia SNe compared to $J-H$ or $H-K$. We show that the $V-K$ color evolution of an ensemble of objects (SNe 1972E, 1980N, 1981B, 1981D, 1983R, and 1999cp) implies that there is a universal relationship for Type Ia SNe with a range of Δ values. Furthermore, because the SN 1998bu data match the “unreddened” color curve by applying a simple arithmetic offset, the offset from one locus to the other is a direct measure of the $V-K$ color excess. A measure of $E(V-K)$ leads directly to A_V with an accuracy equal to or better than that derived solely from B and V data. $V-H$ and $V-J$ colors give similar results.

2. Observations

Supernova 1999aa in NGC 2595 was independently discovered with three different telescopes from 11 to 13 February 1999 UT (Arbour 1999; Qiao et al. 1999; Nakano & Kushida 1999). Filippenko, Li, & Leonard (1999) obtained a spectrum on 12 February UT and noted that it was a peculiar Type Ia supernova very similar to SN 1991T.

SN 1999cl was discovered by Papenkova et al. (1999) on 29 May 1999 UT, roughly 18

days (according to our subsequent analysis) before maximum. Spectra obtained on June 4.2 UT indicated that this SN was highly reddened by dust, with an approximate color excess of $E(B-V) = 1.0$ (Garnavich et al. 1999). This SN occurred in NGC 4501 (= M 88), an SBb/Sc galaxy in the Virgo cluster (Tully 1988). Given this galaxy’s observed axial ratio of roughly 2:1, we view it from an angle of roughly 30 degrees from side-on. As a result, the extreme reddening of the SN is more likely caused by dust local to the SN’s environment rather than by the more uniformly distributed dust in the plane of the galaxy.

SN 1999cp in NGC 5468 was discovered by King & Li (1999) on 18 June UT. A spectrum by Jha et al. (1999a) indicated that it was a Type Ia SN well before maximum light.

We have obtained infrared photometry of these three SNe with the Apache Point Observatory (APO) 3.5-m telescope using GRIM II, which has a 256×256 pixel HgCdTe NICMOS-3 detector. We have obtained optical BVRI photometry with the APO 3.5-m using the facility CCD camera SPIcam, which contains a backside illuminated SITe 2048 \times 2048 array. Additionally, we have obtained CCD photometry with the University of Washington’s Manastash Ridge Observatory (MRO) 0.76-m telescope using a 1024 \times 1024 Ford Aerospace array.

We reduced all our optical data and much of our infrared data with the **IRAF** data reduction package. This first involved subtracting the bias frames, constructing sky flats with the median of three or more sky frames per filter per night, then flattening and trimming the frames. We determined the instrumental magnitudes as aperture magnitudes, using **phot** within the **apphot** package. Calibration of the data was done within the **photcal** package, in particular with **mknobsfile**, **fitparams**, and **evalfit**. As mentioned in §1.1, unless one has images in all relevant filters of the galaxy in question, one cannot carry out image subtraction photometry until template images are obtained a year or more

after the explosion of a SN. From an inspection of Digital Sky Survey images of the host galaxies of SNe 1999aa, 1999cl, and 1999cp we see no serious problems in carrying out aperture photometry of these objects. We agree, however, that images of the host galaxy of SN 1999cl in particular should be obtained in the future to determine if image subtraction significantly changes the data.

The optical photometry is tied to standard stars of Landolt (1992). From data taken on multiple photometric nights we have derived photometric sequences in the field of each supernova (Figs. 2 through 5; Tables 1, 3 and 5). Using differential magnitudes of the field stars with respect to each other, we found no evidence for variability of the field stars to a level of constancy of ± 0.03 mag or better per night. Observations of the brighter field stars on the photometric nights can then give mean values which have very small internal errors.

Typically, we reduced the optical photometry of a SN with the magnitudes and colors of 4 demonstrably constant field stars near the SN; this usually included the brightest field stars so long as they were not located near the edge of the array or near cosmetic defects. Using secondary “standards” within the frame of a SN allows frames taken under non-photometric conditions to be used. Since the in-frame differential photometry was weighted by the reciprocals of the squares of the errors, the calibration of the SN photometry is primarily dependent on the brightest field stars used as local standards. Including several (or many) more faint field stars for the calibration does not significantly improve the results for the SN.

Our optical photometry of SNe 1999aa, 1999cl, and 1999cp are given in Tables 2, 4, and 6 (as nightly means). The uncertainties, given in parentheses, take into account the photon statistics of the raw data, the uncertainties of the V magnitudes and colors of the photometric sequences, and the uncertainties in the transformation coefficients to the BVRI system.

The infrared photometry of SNe 1999aa, 1999cl, and 1999cp given in Table 7 (as nightly means) are tied to standards of Hunt et al. (1998). Our K-band photometry was actually taken in a K' filter, which has a shorter effective wavelength than the regular $2.2\ \mu\text{m}$ filter. Wainscoat & Cowie (1992), who designed this filter to give greater signal-to-noise ratios for infrared imaging, give the transformation: $K' - K = (0.22 \pm 0.03) (H - K)$. To reduce our data we first transformed the K-band values of the Hunt et al. standards used to K' . We then derived K' values for our SNe. Finally, we transform those data using: $K = 1.282 K' - 0.282 H$. In the case of SN 1999aa we did not take H-band data, but used instead the mean $H - K$ vs. age relation given by Elias et al. (1985). At the time this object was observed, the implied differences of K and K' were less than 0.02 mag.

As in the case of the optical photometry, the infrared data were not always taken under photometric conditions. Sometimes it was necessary to use observations of field stars within the SN frames or the core of the host galaxy as secondary standards, whose magnitudes were fixed with observations of infrared standards on photometric nights. Given the greater difficulty in taking and calibrating infrared data, compared to optical photometry, the true uncertainties may be twice as large as the values given in Table 7.

In addition to our own data for SN 1999aa, 1999cl, and 1999cp, we used optical photometry of SN 1972E (Ardeberg & de Groot 1983), 1980N and 1981D (Hamuy et al. 1991), 1981B (Buta & Turner 1983), 1983R (Tsvetkov 1988), and 1998bu (Jha et al. 1999b). Infrared photometry of these SNe is given by Elias et al. (1981, 1985), Mayya et al. (1998), Jha et al. (1999b), and Meikle (1999). We only use two nights' data for SN 1972E, nights on which the infrared data were obtained with the Palomar 200-inch telescope; infrared data taken on other nights with a 0.6-m telescope are much less accurate. Optical photometry for these other objects can be fit with light curve templates derived with Δ values ranging from -0.38 to $+0.20$.

One can construct V-band templates using the MLCS V-band vectors to determine what the V magnitude of a SN was at the times that any infrared data were taken. This is how we determined the V–J, V–H, and V–K colors of SNe 1999aa, 1999cl, 1999cp and the just-mentioned other SNe. Because of the smoothness of V-band light curves near the time of light maximum (see e.g. Riess et al. 1999), in many cases this V-band interpolation involves uncertainties comparable to the internal error of the V-band photometry, ± 0.03 mag or less.

3. Discussion

In Table 8 we give the MLCS fits to the optical photometry of SNe 1999aa, 1999cl, and 1999cp.

SN 1999aa was an overluminous, slow decliner, with $\Delta = -0.47$. This is in accord with the notion that its pre-maximum spectrum was similar to the canonical slow decliner SN 1991T (Lira et al. 1998; Filippenko et al. 1999). From a fourth order polynomial fit to the B-band data we find $\Delta m_{15}(B) = 0.746 \pm 0.024$. In a recent study of 22 Type Ia SNe Riess et al. (1999) found $\Delta m_{15}(B)$ values ranging from 0.86 to 1.93. Thus SN 1999aa is one of the most slowly declining Type Ia SNe known, implying that it is one of most intrinsically bright. Peculiarities in its light curve at optical or infrared wavelengths might not necessarily affect our conclusions based on an ensemble of other objects. MLCS fitting indicates that SN 1999aa is unreddened in its host. The Schlegel et al. (1998) reddening model of our Galaxy indicates that SN 1999aa has been reddened by $E(B-V) = 0.04$ by dust in our Galaxy.

MLCS fitting of the BVRI data of SN 1999cl indicates highly non-standard reddening for this object. The B-band fit and the late I-band points were the most unusual. One

implication would be that the late-time infrared data may not fit. Our photometry indicates that at the time of B-band maximum, the color of the SN was $B-V = 1.23 \pm 0.05$. Given $\Delta = +0.20$ for this object, the implied intrinsic color at light maximum was $B-V = +0.09$. Thus the color excess is $E(B-V) \approx 1.14$.

SN 1999cp is found to be a moderately overluminous object. We find $\Delta = -0.31 \pm 0.10$. It is unreddened in its host. The Galactic reddening at the coordinates of this object is $E(B-V) = 0.025$ (Schlegel et al. 1998).

In Fig. 6 through 8 we show the light curves for SNe 1999aa, 1999cl, and 1999cp. It can readily be seen that the V-band templates allow us to interpolate the V-band data such that we can obtain V minus some-infrared-magnitude at the time that infrared data were taken.

In the lower part of Fig. 9 we show the V–K colors of seven SNe which we assume are essentially unreddened in their host galaxies: SNe 1972E, 1980N, 1981B, 1981D, 1983R, 1999cp, and 1999aa.¹⁰ We have used the Schlegel et al. (1998) reddening maps to correct for reddening of the light in its passage through our Galaxy. Excepting SN 1999aa, all these SNe have $-0.38 \leq \Delta \leq +0.20$. There appears to be a simple linear relation for the run of V–K with time for $t < 6.2$ days after B-band maximum, though admittedly more data for $t < 0$ would be useful. There is another simple linear relation for $t \geq 6.2$ days.¹¹

¹⁰Phillips et al. (1999) adopt non-zero values for the host reddening of SNe 1972E, 1980N, 1981B, and 1981D. However, by applying these reddening corrections, the scatter in our analysis is *increased*. Meikle (1999) carried out his analysis with and without host reddening corrections for these objects.

¹¹There is no *a priori* reason to assume that the color curve could be fit by two linear segments, but that is certainly the simplest approach to adopt.

Clearly, the SN 1999aa points at $t = 20$ and $t = 27$ days are well below the solid line; this would indicate that the K-band light cannot keep up with the V-band light as well as in more “normal” SNe, and in fact the K-band data given in Table 8 indicate that this SN was becoming fainter from one to three weeks after B-band maximum.

In the middle section of Fig. 9 we include the data of SN 1998bu (Mayya et al. 1998, Jha et al. 1999b, Meikle 1999). This object has $\Delta = +0.02$ (Jha et al. 1999b). The 1998bu points prior to $t = 6.2$ days give a slope of -0.0427 ± 0.0059 mag d $^{-1}$. The corresponding “unreddened” points give a slope of -0.0592 ± 0.0085 , which is in reasonable agreement. The 1999bu points after $t = 6.2$ days give a slope of $+0.0652 \pm 0.0038$, while the corresponding “unreddened” points give a slope of $+0.0720 \pm 0.0035$, once again in agreement, within the errors.

Because the slopes of the two linear segments of the “unreddened” color curve match the slopes of the corresponding halves of the SN 1998bu color curve, we assert that the offset is simply $E(V-K)$. Adopting the mean “unreddened” $V-K$ locus, we find that $E(V-K) = 0.979 \pm 0.048$ for SN 1998bu. With Eq. 7 and an equation analogous to Eq. 4, we obtain $A_V = 1.102 \pm 0.061$.¹²

The top set of points in Fig. 9 is data of SN 1999cl. Past $t = 7$ days the final two points deviate from a simple upward translation of the unreddened locus. This may not be so unusual, given that the late-time I-band points were not well fit by the MLCS software. However, the data prior to $t = 7$ days are well fit and indicate $E(V-K) = 1.668 \pm 0.047$, implying $A_V = 1.878 \pm 0.072$.

We find a similar $V-H$ relationship for the six unreddened Type Ia SNe with

¹²Here, and in the discussion that follows, we assume a ± 20 percent uncertainty in the ratio of A_λ/A_V .

$-0.38 \leq \Delta \leq +0.20$ (Fig. 10). The $V-J$ relationship is more complex and exhibits greater scatter (Fig. 11); the first half of the color curve is better fit with a quadratic and the kink in the color curve occurs later, at $t = 10.7$ days. The coefficients of the regressions are given in Table 9.

Once again, we are explicitly assuming that the ensemble of unreddened V *minus* near infrared colors of SNe 1972E, 1980N, 1981B, 1981D, 1983R, and 1999cp represents a universal color curve which is valid for a specific range of Δ values. This assumption is corroborated by the similar (but offset) behavior of the well-observed moderately reddened SN 1998bu.

For SN 1998bu we find $E(V-H) = 0.968 \pm 0.038$ and $A_V = 1.173 \pm 0.068$. Also, we find $E(V-J) = 0.858 \pm 0.067$ and $A_V = 1.195 \pm 0.133$. The weighted mean of our three estimates is $A_V = 1.140 \pm 0.043$. However, because all three estimates use the same adopted V -band values, we do not have three independent estimates of A_V . We therefore adopt $A_V = 1.14 \pm 0.07$ for SN 1998bu. Jha et al. (1999b) obtain $A_V = 0.94 \pm 0.15$ from MLCS fits of BVRI data. Suntzeff et al. (1999) adopt a Galactic reddening of $E(B-V) = 0.025 \pm 0.003$ and obtain a host galaxy reddening of $E(B-V) = 0.34 \pm 0.03$. Assuming $R_V = 3.1$ implies $A_V = 1.132 \pm 0.093$. Meikle (1999) adopts $E(B-V) = 0.35 \pm 0.03$ for the total color excess, implying $A_V = 1.085 \pm 0.093$. Our VJHK analysis is in good agreement with the results based on BV photometry and a Galactic value of R_V .

For SN 1999cl only the early points seem to fit. For $t < 7$ days we find $E(V-H) = 1.435 \pm 0.047$, giving $A_V = 1.739 \pm 0.094$. Also, we adopt $E(V-J) = 1.311 \pm 0.071$, giving $A_V = 1.826 \pm 0.176$. The weighted mean of the VJHK analysis gives $A_V = 1.826 \pm 0.054$. As in the SN 1998bu result, the true uncertainty will be larger. We shall adopt $A_V = 1.83 \pm 0.20$.

As mentioned above, $E(B-V) \approx 1.14$ for SN 1999cl. If $R_V = 3.1$ in this galaxy, then

$A_V = 3.53$, significantly different than our result of $A_V = 1.83 \pm 0.20$. $A_V = 1.83$ and $R_V = 3.1$ would imply that $E(B-V) = 0.59$ and that the intrinsic color of this SN at light maximum was $B-V = 0.64$. However, that contradicts the implied intrinsic color at light maximum of $B-V = +0.09$ for a SN with $\Delta = +0.20$. Another alternative would be that $R_V = 1.83 / 1.14 \approx 1.6$, which strikes us as unrealistic if the composition of the dust in M 88 is anything like that of dust in our Galaxy. Cardelli et al. (1989) indicate that R_V can be as low as 2.60 in our Galaxy, while Riess et al. (1996b) give $R_V = 2.55 \pm 0.30$ as the best reddening ratio applicable to Type Ia SNe. $R_V \approx 1.6$ would mean very small dust grains that would highly redden the light.

From the MLCS V-band fit for SN 1999cl we adopt $V_{max} = 13.68 \pm 0.08$. $\Delta = +0.20$ implies that $M_V \approx -19.14$, for which we adopt an uncertainty of ± 0.3 mag. With $A_V = 1.83 \pm 0.20$, the implied distance is $15.8_{-2.5}^{+2.9}$ Mpc for SN 1999cl and its host, M 88. This is in agreement with modern estimates of the distance to the Virgo cluster (Pierce, McClure, & Racine 1992; Ferrarese et al. 1996; Gibson et al. 1999). Given that M 88 is 2.0 degrees from M 87 (which can be considered the core of the Virgo cluster) the projected distance of M 88 from M 87 is 0.5 Mpc. Thus, in spite of all the uncertainties in photometry reduction, light curve fitting, and reddening ratios, the analysis of rather scanty visual and infrared data of SN 1999cl gives reassuring confirmation that this object is at the “correct” distance.

We note in passing the work of Tripp & Branch (1999, and references therein) on the question of a “second parameter” (i.e. a descriptor for Type Ia SNe in addition to the decline rate). SN models (Höflich & Khokhlov 1996; Nomoto et al. 1997) suggest that the luminous slow decliners may be double degenerate explosions; putting two logs in the fireplace can give a brighter fire that lasts longer. We surmise that the second parameter may be related to the contribution of a particular species (such as silicon) to the opacity of the explosion. A second parameter might explain the very low values of R_V obtained for

SNe like 1999cl. It might also explain deviations from our color curves such as the late time behavior of SN 1999cl and the early time behavior of SN 1991T, which exhibited a V–K “excess” of ≈ 1.5 mag at $t = -11.3$ days (see Meikle 1999).

The existence of well behaved V-band light curves (e.g. from MLCS) and V *minus* infrared color relations implies the existence of infrared light curve templates. In Fig. 12 we show the predicted K-band light curve templates for the range of Δ implied by the unreddened locus in Fig. 9. In Fig. 13 we show the J-, H-, and K-band light curve templates for the fiducial Type Ia SN with $\Delta = 0$. These infrared light curve templates are also listed in Table 10 and may be considered an improvement on those based solely on the data given by Elias et al. (1981, 1985).

4. Conclusions

Using new data and data from the literature, we have outlined a method for determining the V-band extinction towards Type Ia SNe. For SNe with $-0.38 \leq \Delta \leq +0.20$ there appears to be a universal evolution of V *minus* infrared colors from (at least) 9 days before B-band maximum until 27 days after B-band maximum. The slow decliner SN 1999aa (with $\Delta = -0.47$) did not exhibit the same color evolution as six other Type Ia SNe unreddened in their hosts.

If the V *minus* infrared color relations discussed here are indeed universal, the implication is that one can determine A_V for a Type Ia SN using an interpolated V-band light curve and a small amount of infrared photometry obtained between $-9 \leq t \leq +27$ days.

Our VJHK analysis of the moderately reddened SN 1998bu gives a value of $A_V = 1.14 \pm 0.07$, in excellent agreement with (and a possible improvement on) the results from

optical photometry alone.

We were led to consider this method for determining A_V owing to the challenging case of SN 1999cl. The optical data available and the infrared data prior to 7 days after light maximum lead to a value of $A_V = 1.83 \pm 0.20$. Along with the V-band maximum and the implied absolute magnitude from the MLCS fits, we obtain a distance to this object of $15.8^{+2.9}_{-2.5}$ Mpc, in agreement with modern estimates of the distance to the Virgo cluster.

We have several recommendations for future work: (1) We should obtain images of M 88 after SN 1999cl has sufficiently faded away so that image subtraction techniques can be used for this object. (2) Unpublished infrared photometry of Type Ia SNe (especially pre-maximum) should be published if there exist decent V-band light curves of such objects. This will allow further tests of the universality of the color relations discussed here. (3) Telescope time committees should schedule infrared observations of Type Ia SNe during dark time as well as bright time so that we have the chance to observe individual objects in the infrared without large gaps in the light curves. (4) Fast decliners (such as SN 1991bg and 1999da, which occurred in elliptical galaxies) should be observed in the infrared as well as the optical. (5) More unreddened slow decliners should be observed from $-9 \leq t \leq +27$ days to see how their behavior differs from the more normal Type Ia SNe. Given that there are families of BVRI light curves, it would not be surprising if there are families of V *minus* infrared color curves. (6) The next generation of MLCS and other light curve fitting algorithms should use optical *and* infrared data.

We thank Arne Henden (USNO) for photometric calibrations of the NGC 5468 field for SN 1999cp, which augmented our own calibration. Some of the raw data for SN 1999cl and 1999cp were obtained by John Armstrong, Guillermo Gonzalez, Chris Laws, and

Armin Rest. Brian Skiff kindly determined the coordinates of the stars of the photometric sequences. We thank Craig Hogan and Brent Tully for useful discussions. Bradley Schaefer read a previous version of the paper and gave us much appreciated encouragement to proceed. Finally, we thank Peter Meikle for very useful discussions and for making the 1998bu data available.

REFERENCES

Arbour, R. 1999, IAUC No. 7108

Ardeberg, A., & de Groot, M. 1983, A&A, 28, 295

Buta, R. J., & Turner, A. 1983, PASP, 95, 72

Cardelli, J. H., Clayton, G. C., & Mathis, J. S. 1989, ApJ, 345, 245

Elias, J. H., Frogel, J. A., Hackwell, J. A., & Persson, S. E. 1981, ApJ, 251, L13

Elias, J. H., Matthews, K., Neugebauer, G., & Persson, S. E. 1985, ApJ, 296, 379

Ferrarese, L., Freedman, W., Hill, R. J., et al. 1996, ApJ, 464, 568

Filippenko, A. V., Li, W. D., & Leonard, D. C. 1999, IAUC No. 7108

Frogel, J. A., Gregory, B., Kawara, K., Laney, D., Phillips, M. M., Terndrup, D., Vrba, F., and Whitford, A. E. 1987, ApJ, 315, L129

Garnavich, P., Jha, S., Kirshner, R., & Challis, P. 1999, IAUC No. 7190

Gibson, B. K., et al. 1999, astro-ph/9908149

Hamuy, M., Phillips, M. M., Maza, J., Wischnjewsky, M., Uomoto, A., Landolt, A., & Khatwani, R. 1991, AJ, 102, 208

Hamuy, M., Phillips, M. M., Schommer, R. A., Suntzeff, N. B., Maza, J., & Avilés, R. 1996, AJ, 112, 2391

Hernandez, M., et al. 2000, in preparation

Höflich, P., & Khokhlov, A. 1996, ApJ, 457, 500

Hunt, L. K., Mannucci, F., Testi, L., Migliorini, S., Stanga, R. M., Baffa, C., Lisi, F., & Vanzi, L. 1998, AJ, 115, 2594

Jha, S., et al. 1999a, IAUC No. 7206

Jha, S. et al. 1999b, astro-ph/9906220

King, J. Y., & Li, W. D. 1999, IAUC No. 7205

Krisciunas, K., Stubbs, C., Diercks, A., et al. 1999, BAAS, in press

Landolt, A. U. 1992, AJ, 104, 340

Leibundgut, B., Kirschner, R. P., Phillips, M. M., et al. 1993, AJ, 105, 301

Lira, P. 1995, Master's thesis, Univ. of Chile

Lira, P., Suntzeff, N. B., Phillips, M. M., et al. 1998, AJ, 115, 234

Mayya, Y. D., Puerari, I., & Kuhn, O. 1988, IAUC No. 6907

Meikle, P. & Hernandez, M. 1999, J. Ital. Astron. Soc., in press (astro-ph/9902056)

Meikle, W. P. S. 1999, MNRAS, in press (astro-ph/9912123)

Nakano, S., & Kushida, R. 1999, IAUC No. 7109

Nomoto, K., Iwamoto, K., & Kishimoto, N. 1997, Science, 276, 1378

Papenkova, M., Filippenko, A. V., & Treffers, R. R. 1999, IAUC No. 7185.

Perlmutter, S., Gabi, S., Goldhaber, G., et al. 1997, ApJ, 483, 565

Phillips, M. M., Phillips, A. C., Heathcote, S. R., et al. 1987, PASP, 99, 592

Phillips, M. M. 1993, ApJ, 413, L105

Phillips, M. M., Lira, P., Suntzeff, N. B., Schommer, R. A., Hamuy, M., & Maza, J. 1999, astro-ph/9907052

Pierce, M. J., McClure, R. D., & Racine, R. 1992, ApJ, 393, 523

Qiao, Q. Y., Wei, J. Y., Qiu, Y. L., & Hu, J. Y. 1999, IAUC No. 7109

Rieke, G. H., & Lebofsky, M. J. 1985, ApJ, 288, 618

Riess, A. G., Press, W. H., & Kirshner, R. P. 1996a, ApJ, 473, 88 (RPK)

Riess, A. G., Press, W. H., & Kirshner, R. P. 1996b, ApJ, 473, 588

Riess, A. G., Filippenko, A. V., Challis, P., et al. 1998, AJ, 116, 1009

Riess, A. G., Kirshner, R. P., Schmidt, B. P., et al. 1999, AJ, 117, 707

Schaefer, B. E. 1995, ApJ, 450, L5

Schlegel, D. J., Finkbeiner, D. P., & Davis, M. 1998, ApJ, 500, 525

Sneden, C., Gehrz, R. D., Hackwell, J. A., York, D. G., & Snow, T. P. 1978, ApJ, 223, 168

Suntzeff, N. B., Phillips, M. M., Covarrubias, R., et al. 1999, AJ, 117, 1175

Tripp, R., & Branch, D. 1999, astro-ph/9904347

Tsvetkov, D. Yu. 1988, Sov. Astron., 32, 72

Tully, R. B. 1988, *Nearby Galaxies Catalog*, Cambridge Univ. Press

Wainscoat, R. J., & Cowie, L. L. 1992, AJ, 103, 332

Table 1. NGC 2595 Photometric Sequence for SN 1999aa

Star	α (2000)	δ (2000)	V	B-V	V-R	V-I
2	8:27:43.3	+21:29:52	16.762 (0.010)	0.849 (0.015)	0.434 (0.011)	0.847 (0.012)
3	8:27:38.2	+21:29:55	15.079 (0.009)	0.683 (0.010)	0.373 (0.008)	0.752 (0.008)
4	8:27:43.4	+21:30:34	20.039 (0.026)	1.620 (0.108)	1.170 (0.038)	2.626 (0.023)
5	8:27:40.7	+21:31:08	18.979 (0.010)	0.753 (0.018)	0.423 (0.010)	0.833 (0.014)
6	8:27:37.3	+21:30:58	16.624 (0.011)	1.070 (0.012)	0.592 (0.012)	1.130 (0.011)
7	8:27:35.2	+21:29:47	18.484 (0.014)	1.403 (0.021)	0.809 (0.015)	1.594 (0.014)
9	8:27:32.5	+21:28:34	18.425 (0.014)	0.529 (0.019)	0.298 (0.010)	0.676 (0.016)
10	8:27:35.7	+21:28:00	18.516 (0.013)	1.533 (0.022)	0.984 (0.010)	2.141 (0.013)
11	8:27:36.9	+21:27:31	18.737 (0.018)	0.937 (0.019)	0.493 (0.021)	1.003 (0.015)
12	8:27:40.8	+21:27:22	15.792 (0.009)	0.844 (0.011)	0.453 (0.008)	0.904 (0.009)

Table 2. BVRI Photometry of SN 1999aa^a

JD - 2,451,000	V	B-V	V-R	V-I
228.5901	14.980 (0.004)	-0.014 (0.005)	-0.057 (0.004)	-0.261 (0.004)
234.6081	14.857 (0.004)	0.077 (0.006)	-0.042 (0.006)	-0.442 (0.005)
238.5953	14.925 (0.005)	0.119 (0.007)	-0.062 (0.005)	-0.545 (0.006)
240.6058	14.978 (0.004)	0.149 (0.006)	-0.072 (0.007)	-0.542 (0.006)
244.6252	15.189 (0.004)	0.211 (0.004)	-0.133 (0.004)	-0.574 (0.004)
249.5977	15.502 (0.004)	0.420 (0.004)	-0.115 (0.004)	-0.383 (0.004)
252.6033	15.650 (0.004)	0.620 (0.004)	-0.020 (0.005)	-0.180 (0.004)
257.6257	15.878 (0.003)	0.912 (0.004)		0.156 (0.004)
263.6145	16.151 (0.006)	1.184 (0.014)	0.312 (0.008)	0.472 (0.013)
265.6119	16.269 (0.005)	1.150 (0.010)	0.343 (0.005)	0.571 (0.006)
274.7846	16.767 (0.011)	1.044 (0.086)		0.533 (0.013)
275.6135	16.796 (0.004)	1.057 (0.006)	0.288 (0.006)	0.525 (0.004)
279.6524	16.934 (0.004)	0.997 (0.005)	0.265 (0.004)	0.463 (0.005)
318.6274	17.900 (0.014)	0.530 (0.020)	0.004 (0.021)	-0.187 (0.037)
322.6412	18.050 (0.044)	0.640 (0.053)	0.052 (0.067)	-0.264 (0.060)

^aThe data were derived with respect to stars 2, 3, 6, and 12 of the NGC 2595 photometric sequence.

Table 3. NGC 4501 Photometric Sequence for SN 1999cl

Star	α (2000)	δ (2000)	V	B-V	V-R	V-I
1	12 31 57.2	+14 26 15	17.372 (0.005)	0.096 (0.003)	0.107 (0.019)	0.163 (0.015)
2	12 31 55.5	+14 26 13	18.450 (0.006)	0.456 (0.007)	0.302 (0.012)	0.616 (0.021)
4	12 31 52.8	+14 23 52	19.234 (0.006)	0.491 (0.012)	0.323 (0.052)	0.710 (0.011)
5	12 31 49.1	+14 23 38	18.584 (0.005)	1.460 (0.021)	0.929 (0.004)	1.838 (0.009)
7	12 31 57.1	+14 28 52	11.879 (0.004)	0.783 (0.020)	0.448 (0.028)	0.817 (0.050)
8	12 32 08.8	+14 28 44	14.687 (0.020)	0.581 (0.030)	0.405 (0.009)	0.729 (0.011)
9	12 31 49.4	+14 21 48	16.293 (0.017)	0.900 (0.078)	0.547 (0.030)	0.986 (0.032)
11	12 32 05.2	+14 23 34	13.628 (0.004)	0.841 (0.008)	0.538 (0.005)	0.988 (0.005)
12	12 32 04.7	+14 23 16	14.970 (0.008)	0.716 (0.022)	0.467 (0.015)	0.864 (0.017)

Table 4. BVRI Photometry of SN 1999cl^a

JD – 2,451,000	Observatory	V	B–V	V–R	V–I
336.6966	APO	14.215 (0.007)	1.069 (0.011)	0.630 (0.012)	0.996 (0.014)
337.7858	APO	14.138 (0.014)	1.072 (0.020)	0.560 (0.023)	0.873 (0.025)
339.7589	MRO	13.932 (0.008)	1.157 (0.023)	0.600 (0.016)	0.919 (0.019)
340.6926	APO	13.902 (0.006)	1.127 (0.009)	0.511 (0.009)	0.772 (0.010)
363.7404	MRO	14.604 (0.010)	2.184 (0.071)	0.780 (0.015)	1.455 (0.016)
365.7448	MRO	14.727 (0.008)	2.027 (0.037)	0.828 (0.015)	1.566 (0.017)
367.7305	MRO	14.768 (0.018)	2.033 (0.177)	0.784 (0.025)	1.647 (0.024)
368.7221	MRO	14.936 (0.023)	2.029 (0.105)	0.934 (0.033)	1.717 (0.032)

^aThe APO data were reduced with respect to stars 1, 2, and 5 of the NGC 4501 photometric sequence, while the MRO data were reduced with respect to stars 7, 8, 11, and 12.

Table 5. NGC 5468 Photometric Sequence for SN 1999cp

Star	α (2000)	δ (2000)	V	B-V	V-R	V-I
1	14 06 28.6	-5 27 33	16.356 (0.005)	0.525 (0.016)	0.356 (0.004)	0.670 (0.005)
2	14 06 29.4	-5 28 54	15.124 (0.018)	0.133 (0.006)	0.132 (0.004)	0.271 (0.004)
3	14 06 27.3	-5 30 23	14.474 (0.010)	0.534 (0.010)	0.355 (0.007)	0.720 (0.008)
4	14 06 32.3	-5 30 45	15.255 (0.010)	0.626 (0.010)	0.399 (0.012)	
5	14 06 34.3	-5 29 33	16.715 (0.020)	0.610 (0.020)	0.421 (0.047)	0.856 (0.055)
6	14 06 41.6	-5 26 00	14.617 (0.010)	0.961 (0.010)	0.577 (0.007)	1.075 (0.008)
7	14 06 28.2	-5 24 51	16.739 (0.043)	1.044 (0.044)	0.606 (0.006)	1.136 (0.006)
8	14 06 23.4	-5 25 46	15.340 (0.004)	0.706 (0.008)	0.432 (0.004)	0.792 (0.004)

Table 6. BVRI Photometry of SN 1999cp

JD – 2,451,000	Observatory	V	B–V	V–R	V–I
355.7334	MRO	14.671 (0.016)	–0.116 (0.044)	0.127 (0.020)	0.088 (0.023)
365.7721	MRO	14.045 (0.005)	0.006 (0.008)	–0.023 (0.007)	–0.401 (0.013)
367.7459	MRO	14.099 (0.011)	0.100 (0.024)	–0.034 (0.014)	–0.412 (0.018)
368.7429	MRO	14.125 (0.008)	0.078 (0.015)	–0.024 (0.009)	–0.494 (0.015)
383.6373	APO	14.939 (0.004)	0.621 (0.006)	0.003 (0.003)	–0.136 (0.004)

^aThe MRO data were reduced with respect to stars 2, 3, 6, and 8 of the NGC 5468 photometric sequence, while the APO data were reduced with respect to stars 2 and 8.

Table 7. Infrared Photometry

Object	JD - 2,451,000	J	H	K
SN 1999aa	239.82	16.28 (0.04)		15.78 (0.07)
	244.82	17.10 (0.08)		
	252.72	17.00 (0.06)		15.90 (0.05)
	259.59	16.87 (0.04)		15.96 (0.05)
SN 1999cl	337.67	12.96 (0.02)		12.74 (0.02)
	340.65	12.80 (0.02)	12.98 (0.02)	12.58 (0.02)
	341.68	12.89 (0.02)	13.02 (0.02)	12.59 (0.02)
	351.78	14.27 (0.04)	13.29 (0.04)	13.11 (0.06)
	360.63	14.01 (0.02)	12.84 (0.02)	12.70 (0.03)
	367.62	13.49 (0.04)	12.77 (0.04)	12.77 (0.05)
SN 1999cp	354.81	14.88 (0.03)	15.04 (0.07)	14.94 (0.15)
	360.67	14.50 (0.02)	14.77 (0.02)	14.57 (0.06)

Table 8. Multi-color Light Curve Shape Fits

Object	$T(B_{max}) - 2,451,000$	Δ	M_V	A_V	$m - M$
SN 1999aa	232.37 (0.23)	–0.47 (0.08)	–19.80 (0.15)	0.00 (0.15)	34.53 (0.16)
SN 1999cl	345.02 (0.20)	+0.20 (0.3:)	–19.14 (0.3:)	2.00 (0.5:)	30.83 (0.6:)
SN 1999cp	363.62 (0.28)	–0.31 (0.10)	–19.65 (0.10)	0.00 (0.12)	33.56 (0.13)

Table 9. (V - [Near Infrared]) Regression Lines^a

Valid t	Filter	a	b	c	σ
< 10.7	J	-0.654	-0.0964	-0.00288	± 0.062
≥ 10.7	J	-2.897	0.0825	0	± 0.039
< 5.0	H	-0.807	-0.0646	0	± 0.028
≥ 5.0	H	-1.502	0.0739	0	± 0.020
< 6.2	K	-0.657	-0.0592	0	± 0.043
≥ 6.2	K	-1.476	0.0720	0	± 0.018

^aTime t is the number of days since B-band maximum. The least-squares fits are of the form: $V - [J, H, \text{ or } K] = a + bt + ct^2$. σ is the RMS uncertainty of the regression divided by the square root of the number of points used for the fit.

Table 10. Infrared Light Curve Templates

t	M_J	M_H	M_K	M_K	M_K
$\Delta:$	0.0	0.0	-0.38	0.0	+0.20
-9.0	-18.494	-18.289	-18.799	-18.390	-18.203
-8.0	-18.605	-18.384	-18.899	-18.490	-18.304
-7.0	-18.683	-18.450	-18.971	-18.562	-18.376
-6.0	-18.755	-18.516	-19.043	-18.634	-18.448
-5.0	-18.841	-18.602	-19.133	-18.724	-18.538
-4.0	-18.850	-18.615	-19.152	-18.743	-18.557
-3.0	-18.835	-18.613	-19.156	-18.747	-18.561
-2.0	-18.803	-18.599	-19.147	-18.738	-18.547
-1.0	-18.753	-18.572	-19.120	-18.716	-18.519
0.0	-18.686	-18.533	-19.079	-18.683	-18.479
1.0	-18.601	-18.484	-19.027	-18.639	-18.433
2.0	-18.501	-18.424	-18.970	-18.585	-18.378
3.0	-18.385	-18.354	-18.909	-18.520	-18.313
4.0	-18.256	-18.277	-18.845	-18.448	-18.234
5.0	-18.111	-18.190	-18.772	-18.367	-18.145
6.0	-17.954	-18.232	-18.691	-18.279	-18.048
7.0	-17.785	-18.270	-18.699	-18.283	-18.045
8.0	-17.603	-18.302	-18.735	-18.313	-18.069
9.0	-17.411	-18.330	-18.767	-18.339	-18.089
10.0	-17.209	-18.353	-18.798	-18.360	-18.103
11.0	-17.072	-18.373	-18.825	-18.378	-18.112

Table 10—Continued

<i>t</i>	M _J	M _H	M _K	M _K	M _K
12.0	-17.098	-18.390	-18.848	-18.393	-18.118
13.0	-17.122	-18.404	-18.868	-18.406	-18.124
14.0	-17.144	-18.418	-18.887	-18.418	-18.128
15.0	-17.166	-18.431	-18.906	-18.429	-18.130
16.0	-17.186	-18.443	-18.924	-18.439	-18.132
17.0	-17.207	-18.455	-18.938	-18.449	-18.132
18.0	-17.227	-18.467	-18.949	-18.459	-18.133
19.0	-17.249	-18.480	-18.965	-18.470	-18.134
20.0	-17.270	-18.492	-18.984	-18.481	-18.137
21.0	-17.291	-18.504	-19.004	-18.491	-18.141
22.0	-17.313	-18.518	-19.026	-18.503	-18.146
23.0	-17.336	-18.532	-19.048	-18.515	-18.153
24.0	-17.358	-18.546	-19.069	-18.527	-18.158
25.0	-17.381	-18.560	-19.090	-18.539	-18.163
26.0	-17.404	-18.575	-19.110	-18.552	-18.167
27.0	-17.428	-18.590	-19.129	-18.565	-18.173

^aTime *t* is the number of days since B-band maximum. These infrared templates were generated using the regression lines given in Table 9, and assuming that the fiducial Type Ia SN has M_V = -19.34 (Jha et al. 1999).

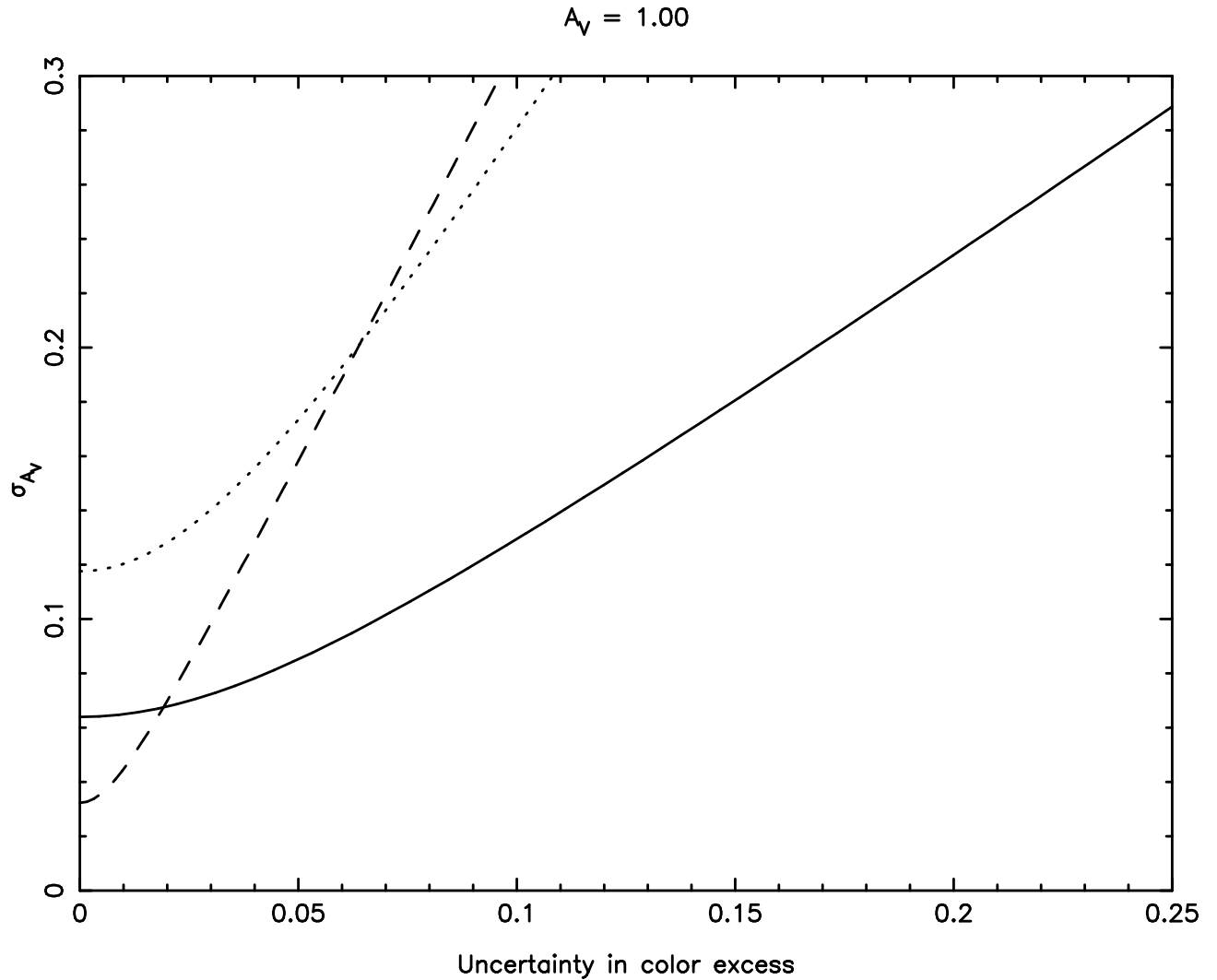


Fig. 1.— The uncertainty in the extinction A_V as a function of the uncertainty of the color excess, for $A_V = 1.00$. Solid line: *worst* case V–K scenario. Dashed line: *best* case B–V scenario. Dotted line: most appropriate B–V case for Type Ia SNe. See text for details.

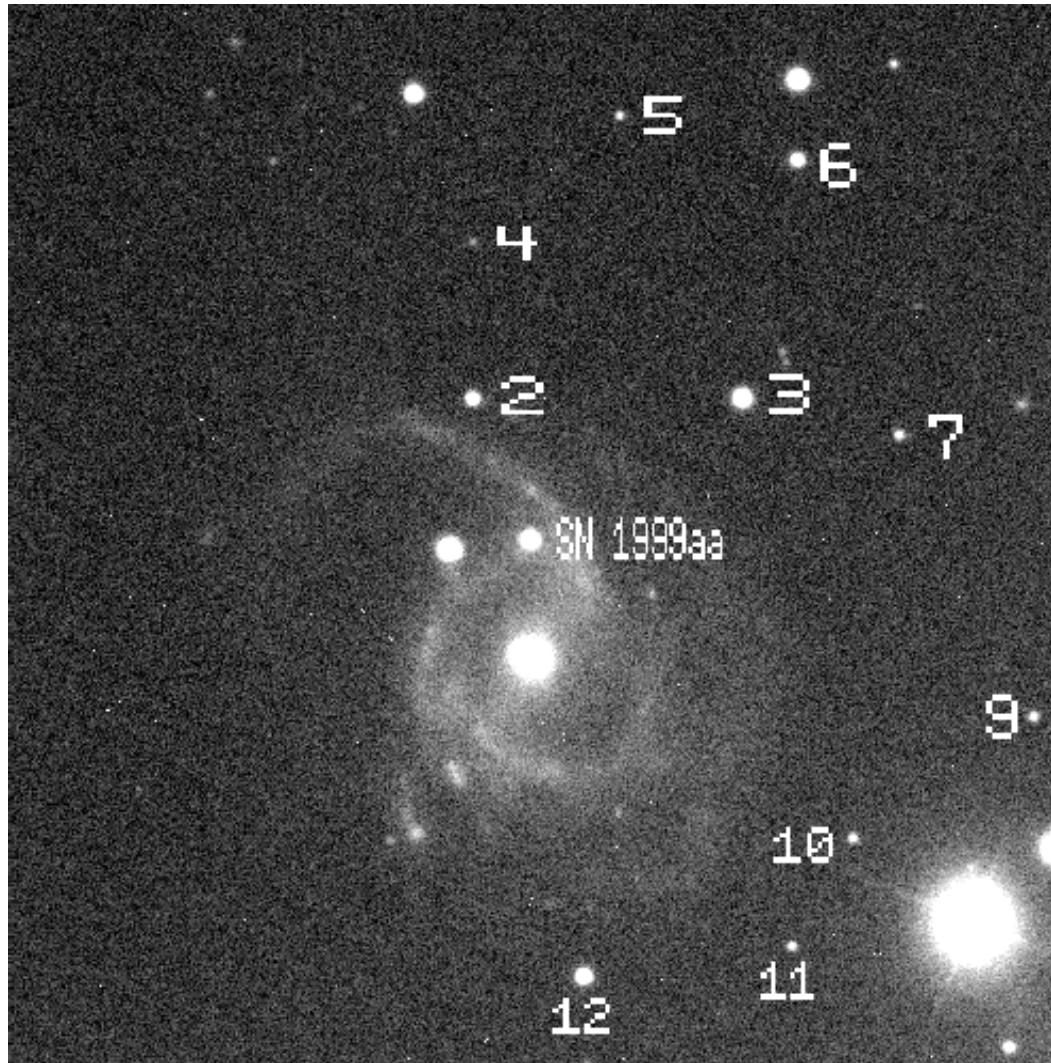


Fig. 2.— A V-band image of NGC 2595 obtained at APO on 19 February 1999 UT, with SN 1999aa and the stars of the photometric sequence indicated. The field is 4.8 arcmin on a side. North is up, east to the left.

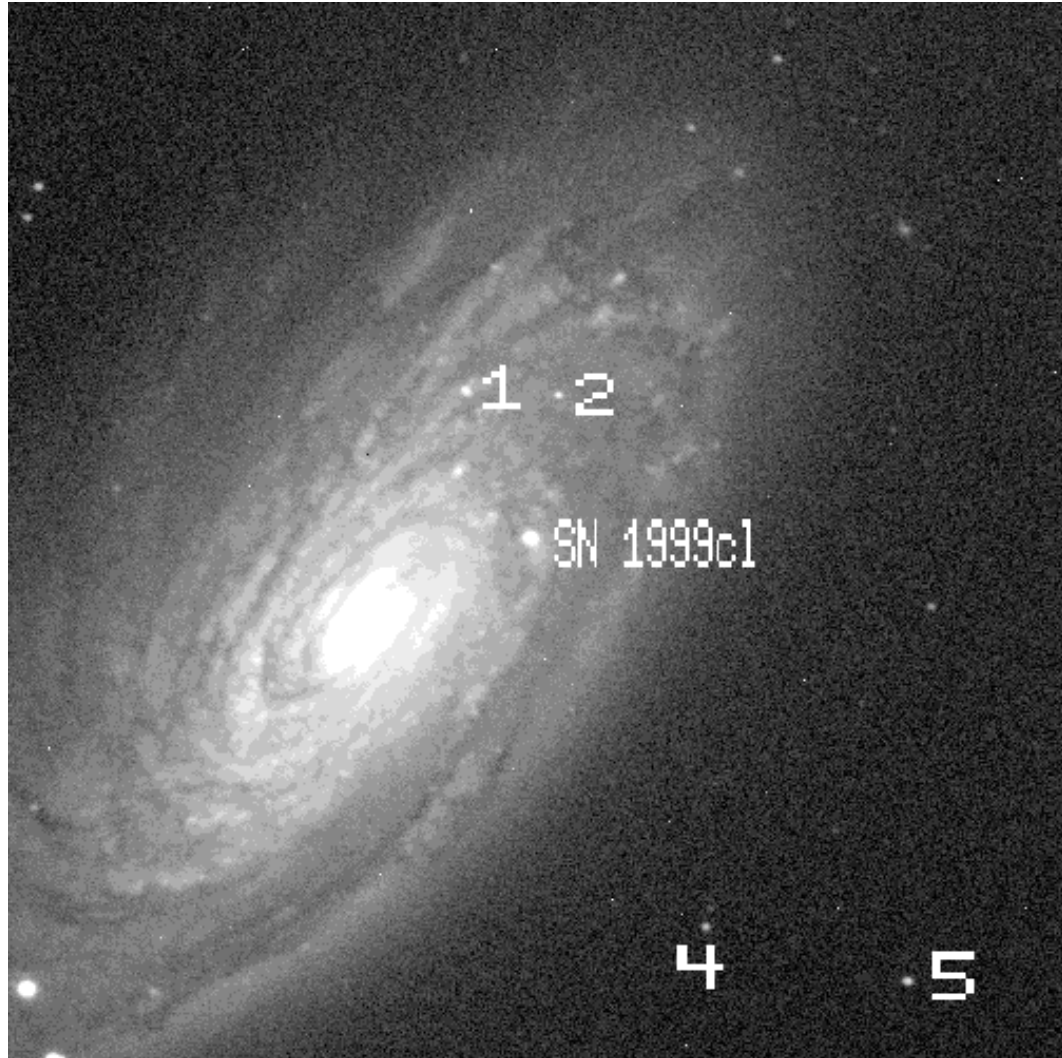


Fig. 3.— A V-band image of NGC 4501 obtained with APO on 11 June 1999 UT, with SN 1999cl and stars 1, 2, 4 and 5 of the photometric sequence indicated. The field is 4.8 arcmin on a side. North is up, east to the left.

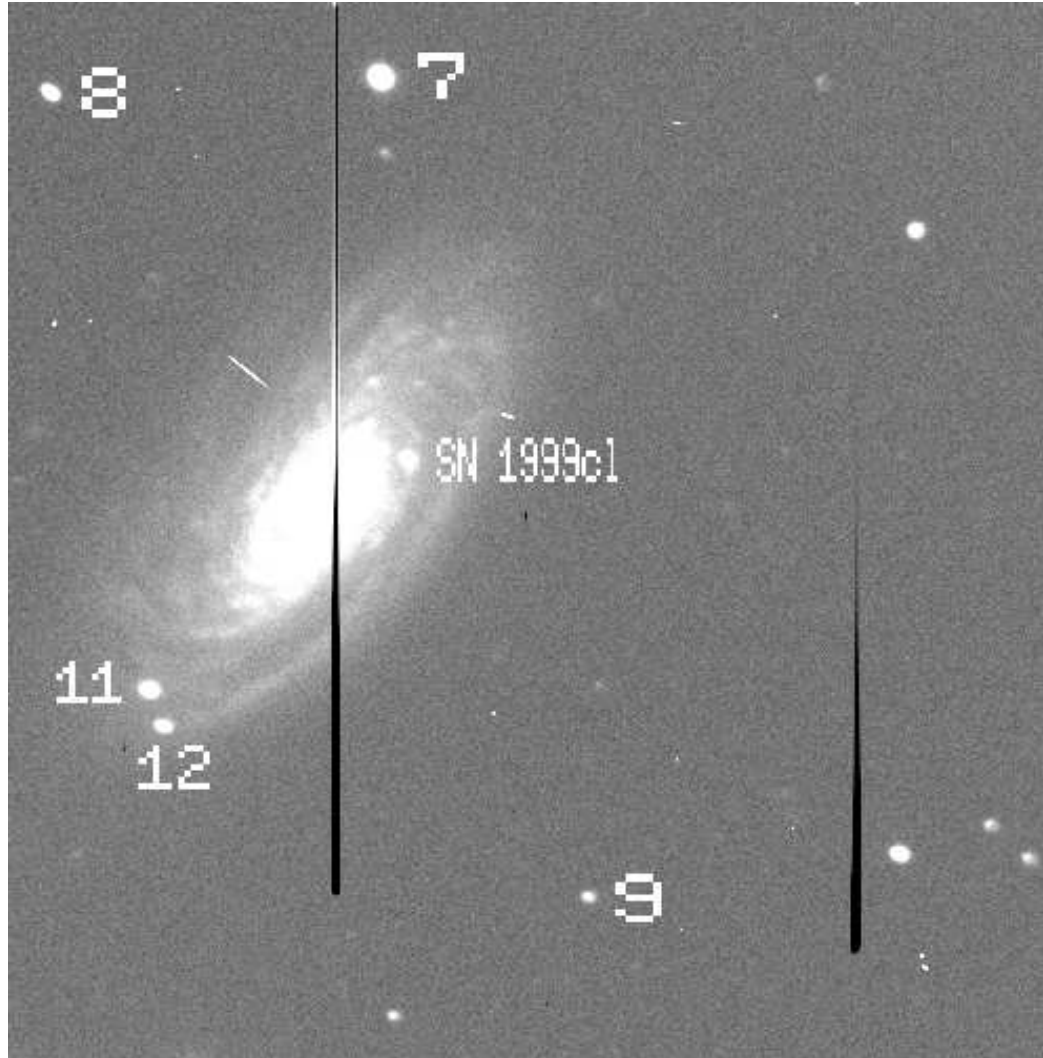


Fig. 4.— A V-band image of NGC 4501 obtained with MRO on 6 July 1999 UT, with SN 1999cl and other stars of the photometric sequence indicated. The field is 11 arcmin on a side. North is up, east to the left.

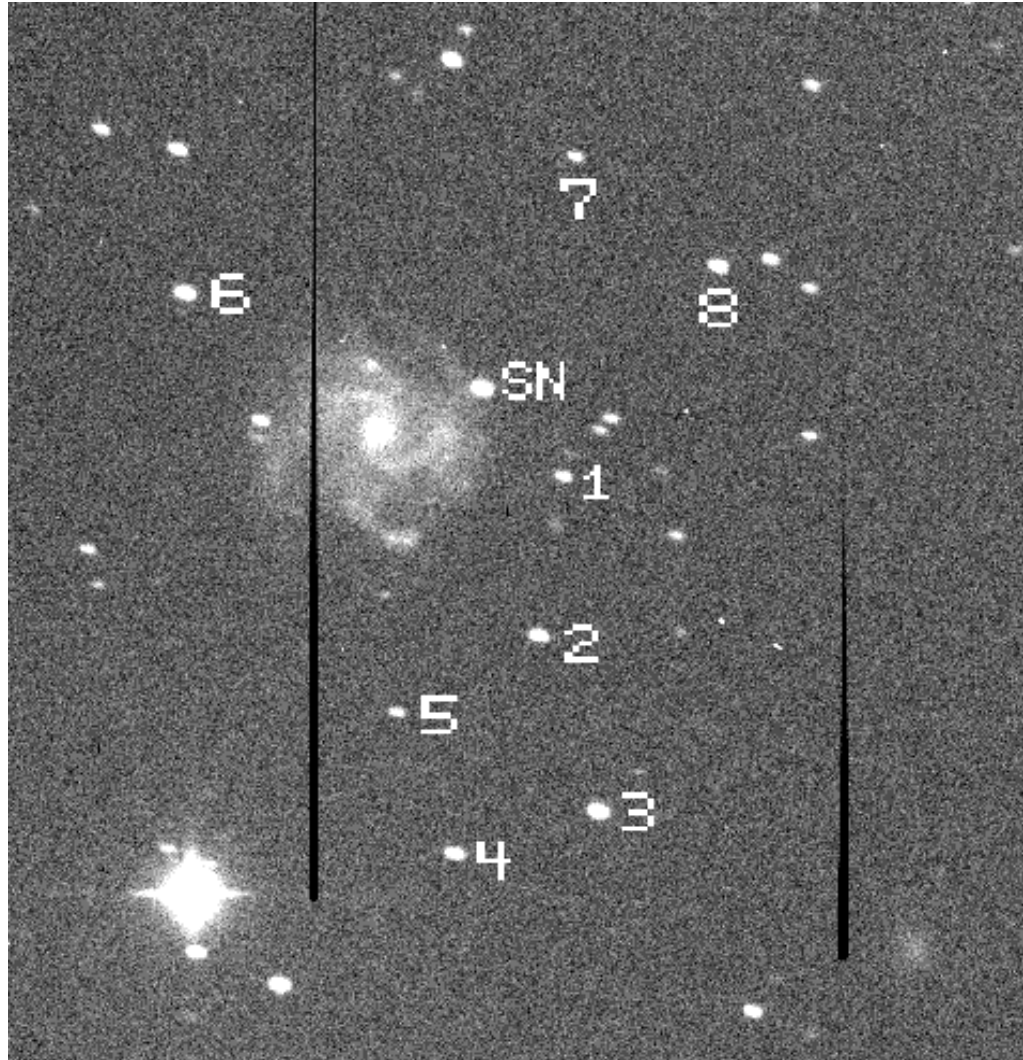


Fig. 5.— A V-band image of NGC 5468 obtained with MRO on 9 July 1999 UT, with SN 1999cp and the stars of the photometric sequence indicated. The field is 11 arcmin on a side. North is up, east to the left.

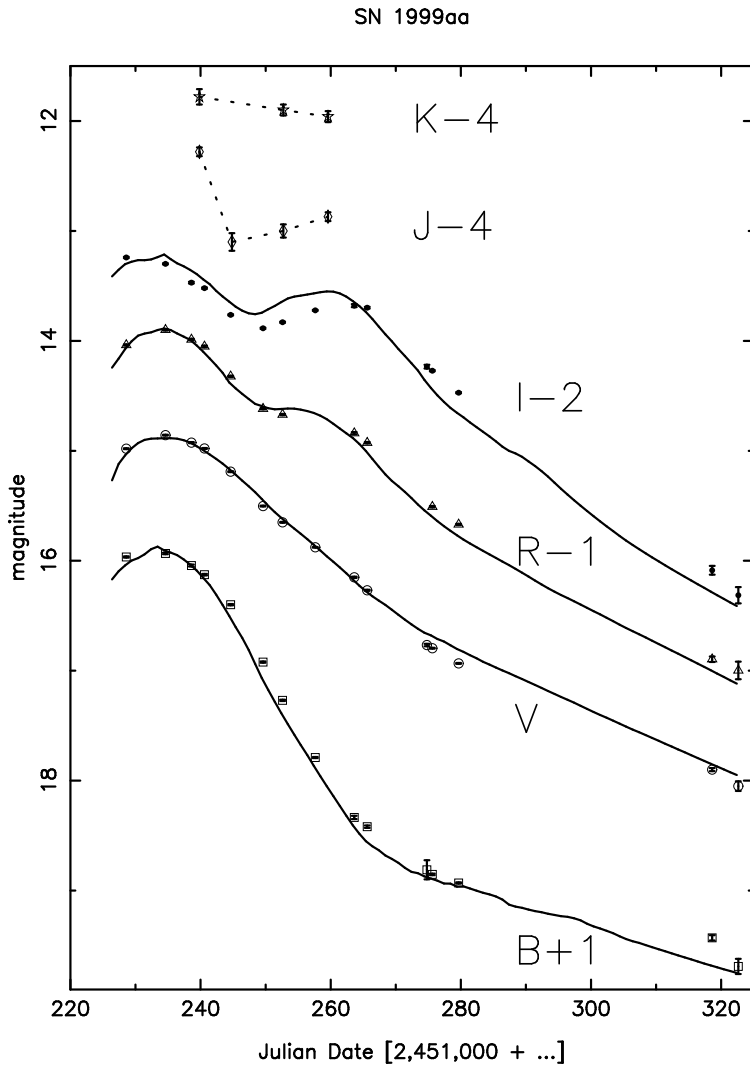


Fig. 6.— BVRIJK photometry of SN 1999aa. The B, R, I, J, and K data have been offset vertically by +1, -1, -2, -4, and -4 magnitudes, respectively. The solid lines are based on MLCS empirical fits with $\Delta = -0.47$.

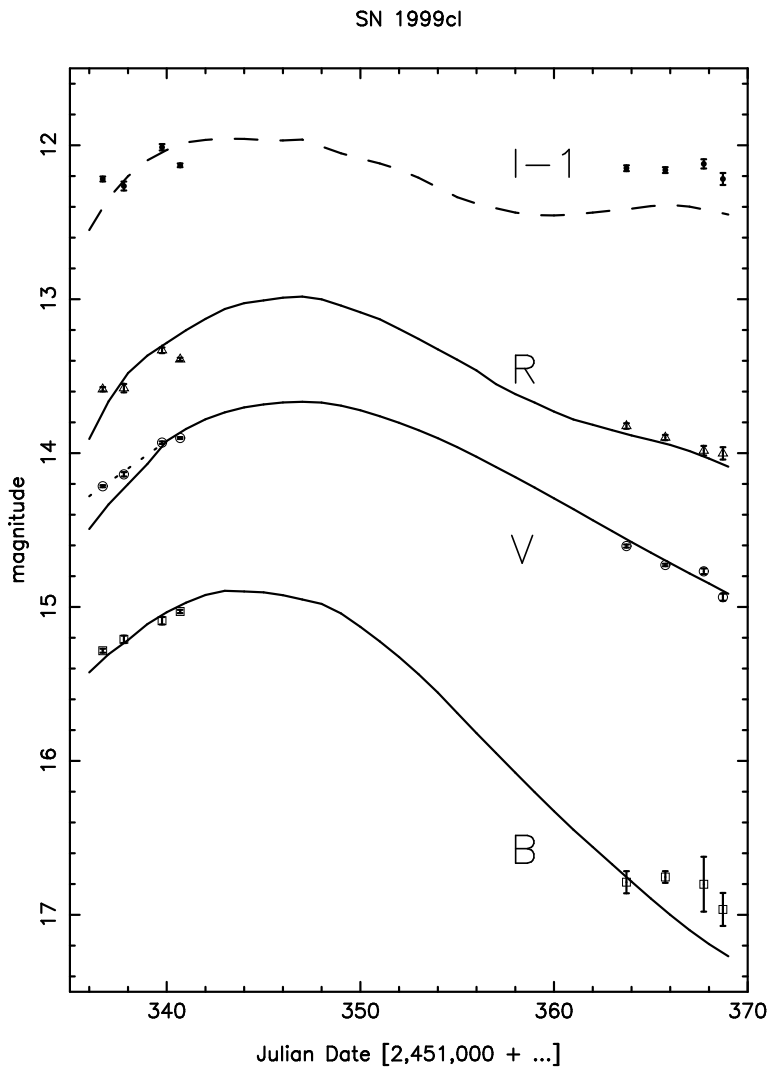


Fig. 7.— BVRI photometry of SN 1999cl. Only the I-band data has been offset (by -1 magnitude). Also shown are the MLCS empirical fits with $\Delta = +0.20$, but clearly the I-band fit is not good at late times. For the purposes of determining V *minus* infrared colors at early times, the dotted line fit to the early points will be used.

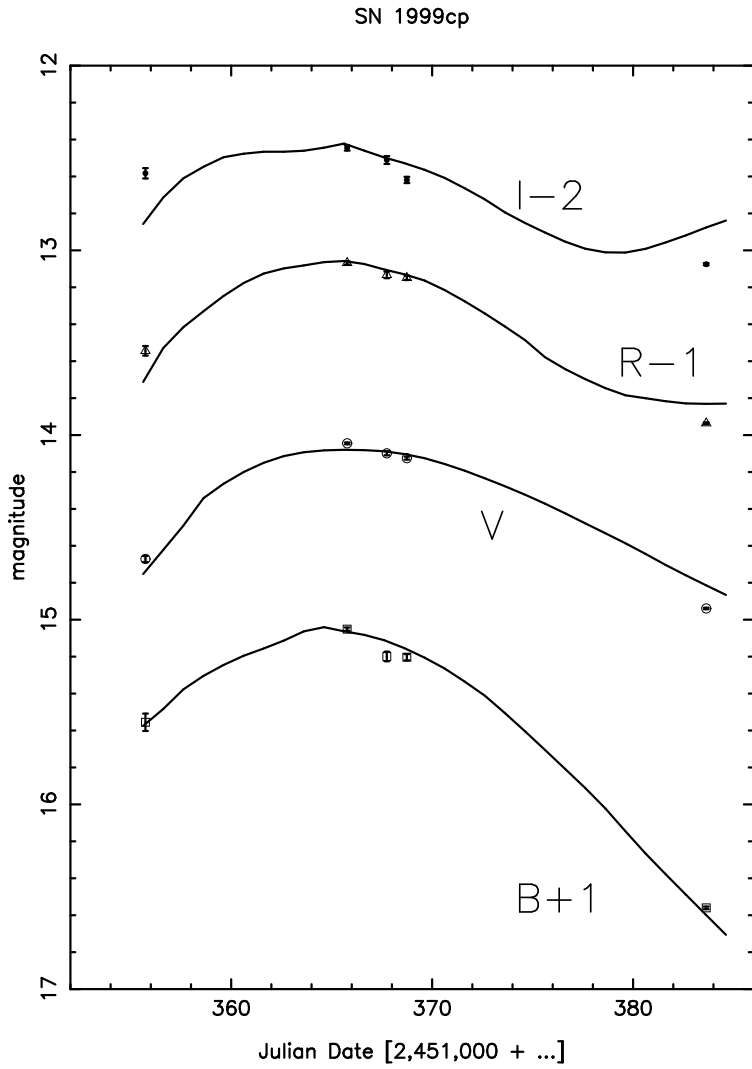


Fig. 8.— BVRI photometry of SN 1999cp. The B, R, and I data have been offset vertically by +1, -1, and -2 magnitudes, respectively. The solid lines are based on MLCS empirical fits with $\Delta = -0.31$.

V-K color evolution of Type Ia supernovae

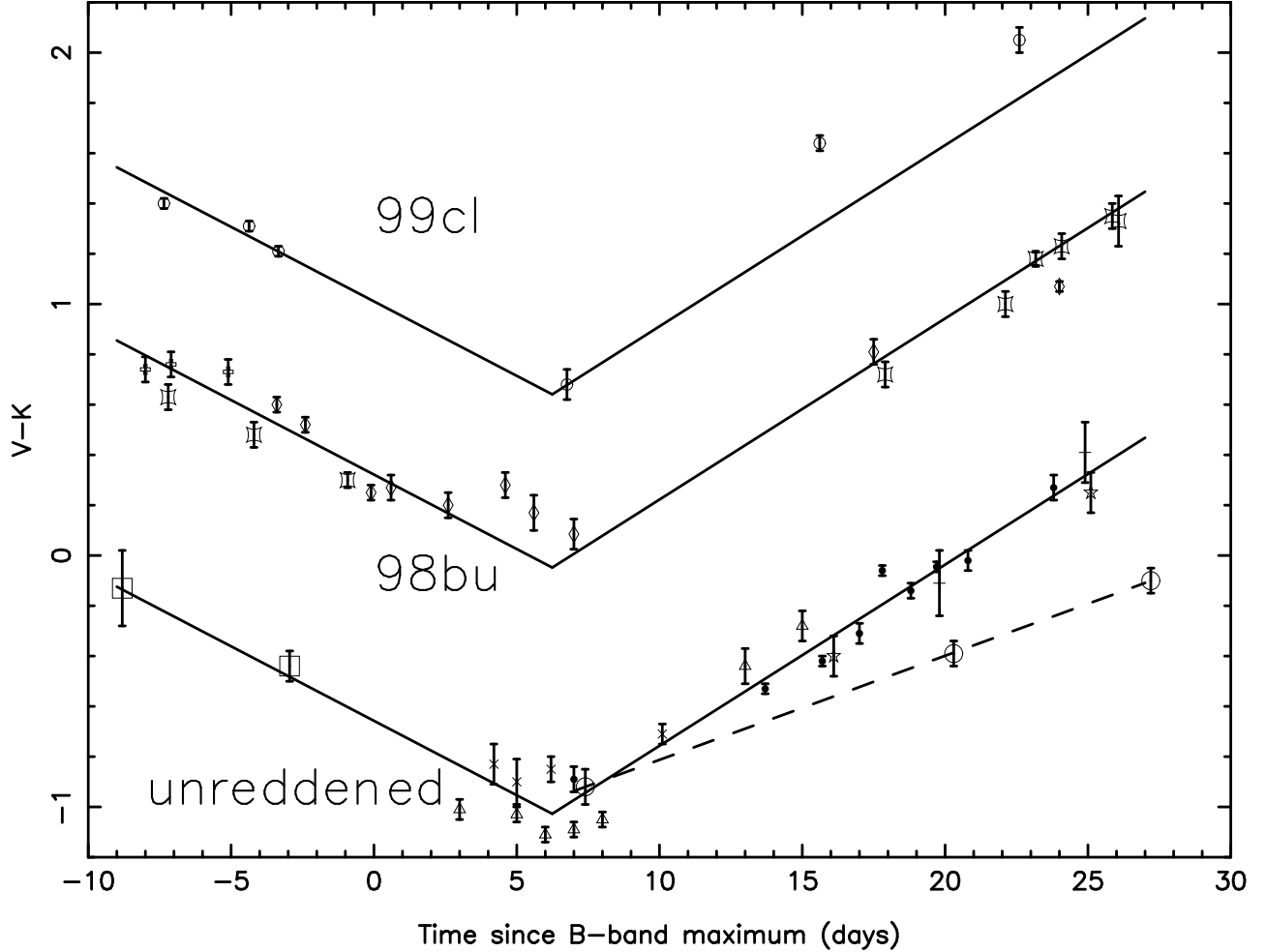


Fig. 9.— V-K color of Type Ia SNe vs. time since B-band maximum. In the bottom locus different points correspond to different objects: SN 1972E (five pointed stars), 1980N (\times 's), 1981B (dots), 1981D (triangles), 1983R (+'s), 1999aa (large open circles), and 1999cp (large open squares); these points have been corrected for reddening in *our* Galaxy according to the reddening model of Schlegel et al. (1998). The SN 1999aa points have been excluded from the solid line fit on the bottom right. In the middle locus we give data of Mayya et al. (1998) as open crosses, Meikle (1999) as diamonds, and Jha et al. (1999b) as pinched in squares. The bottom solid line has been displaced by +0.979 mag to produce the middle fit for SN 1998bu, and has been displaced +1.668 mag to produce the top fit for SN 1999cl.

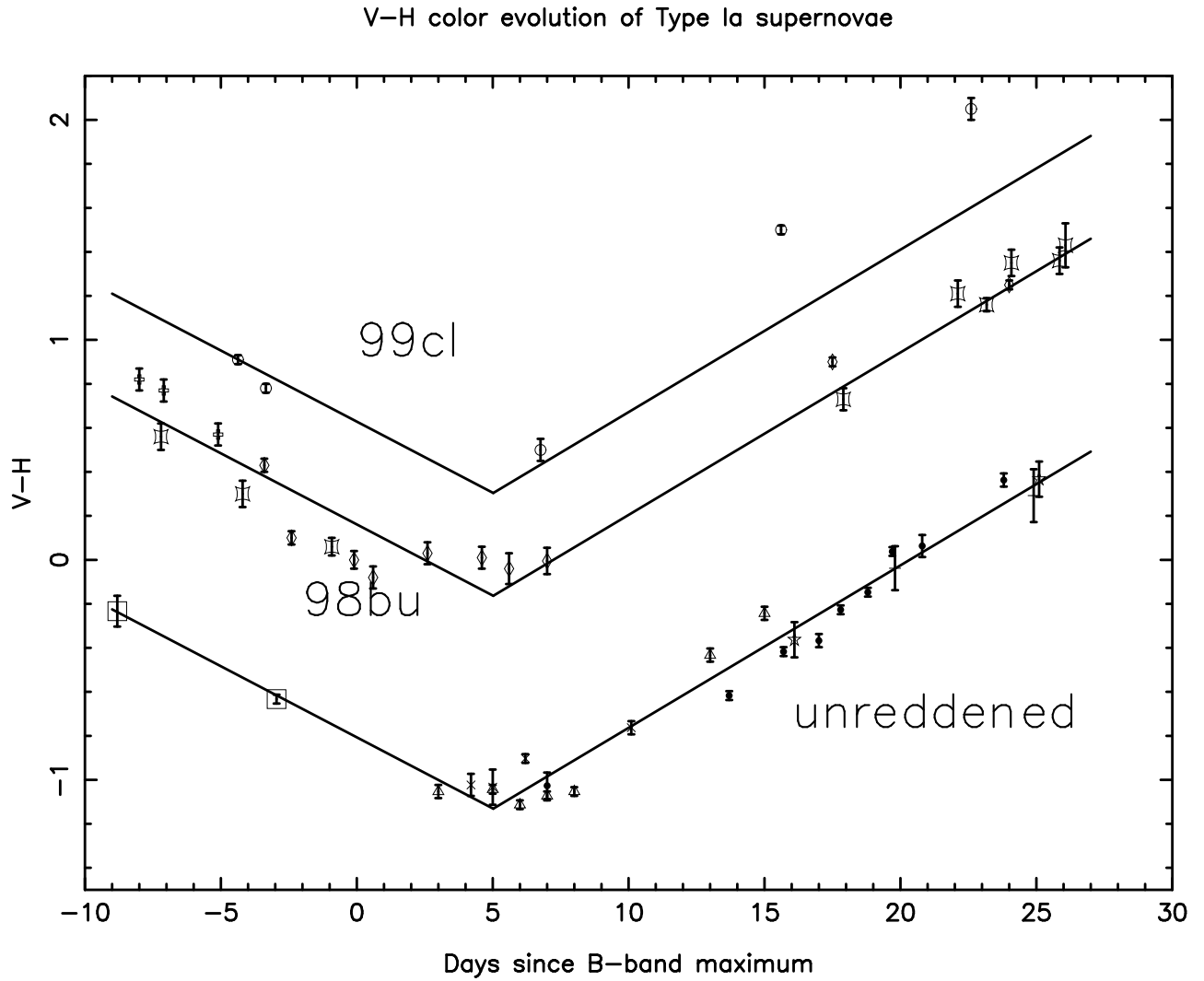


Fig. 10.— V-H color of Type Ia SNe vs. time since B-band maximum. The symbols are the same as in Fig. 9. The bottom locus has been offset by 0.968 mag to produce the middle fit for SN 1999bu, and has been displaced by 1.435 mag to produce the top fit for SN 1999cl.

V–J color evolution of Type Ia supernovae

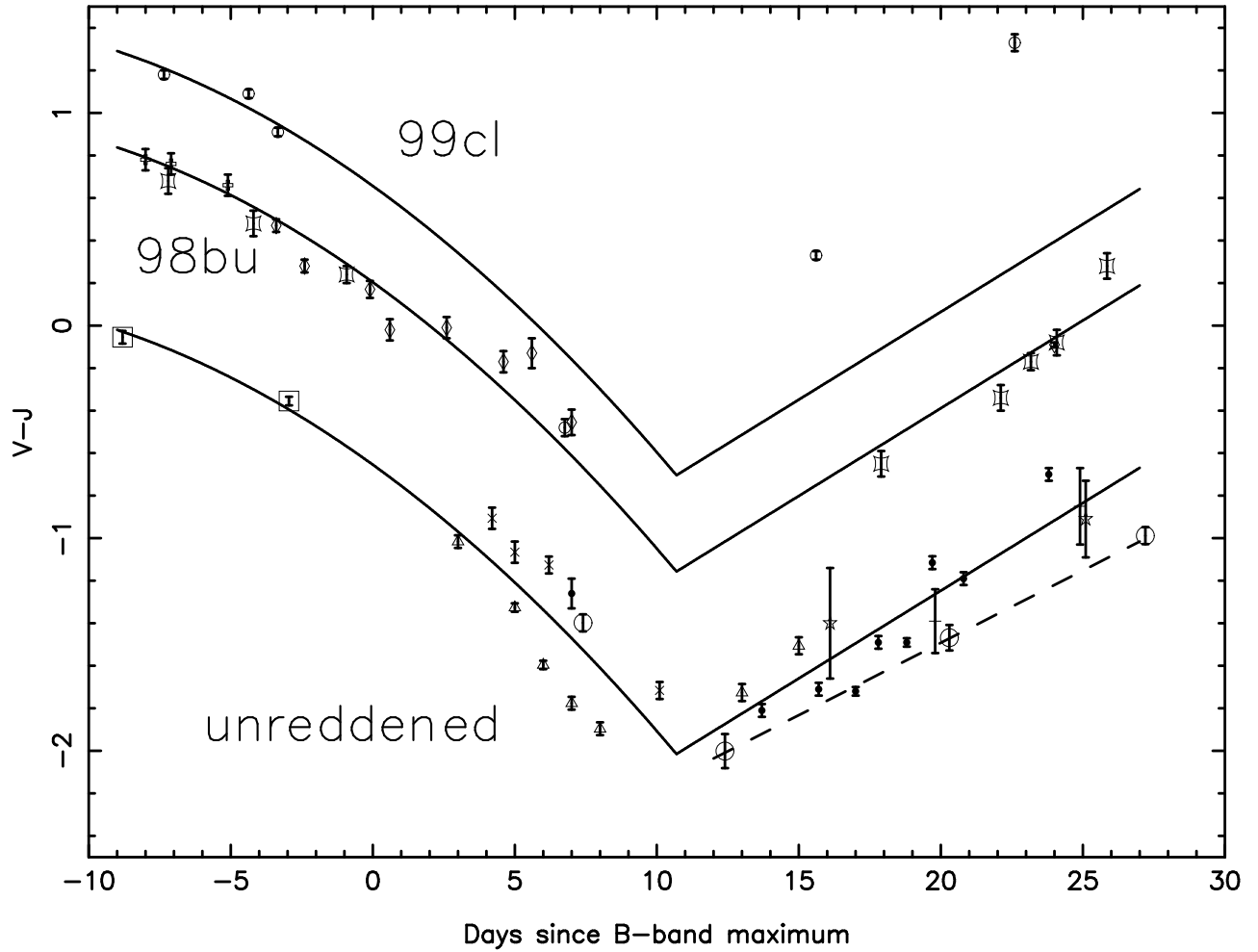


Fig. 11.— V–J color of Type Ia SNe vs. time since B-band maximum. The symbols are the same as in Fig. 9 and 10. The bottom locus has been offset by 0.858 mag to produce the middle fit for SN 1999bu, and has been displaced by 1.311 mag to produce the top fit for the early SN 1999cl points. The points for SN 1999aa (larger open circles) have not been used for the lower solid line fits.

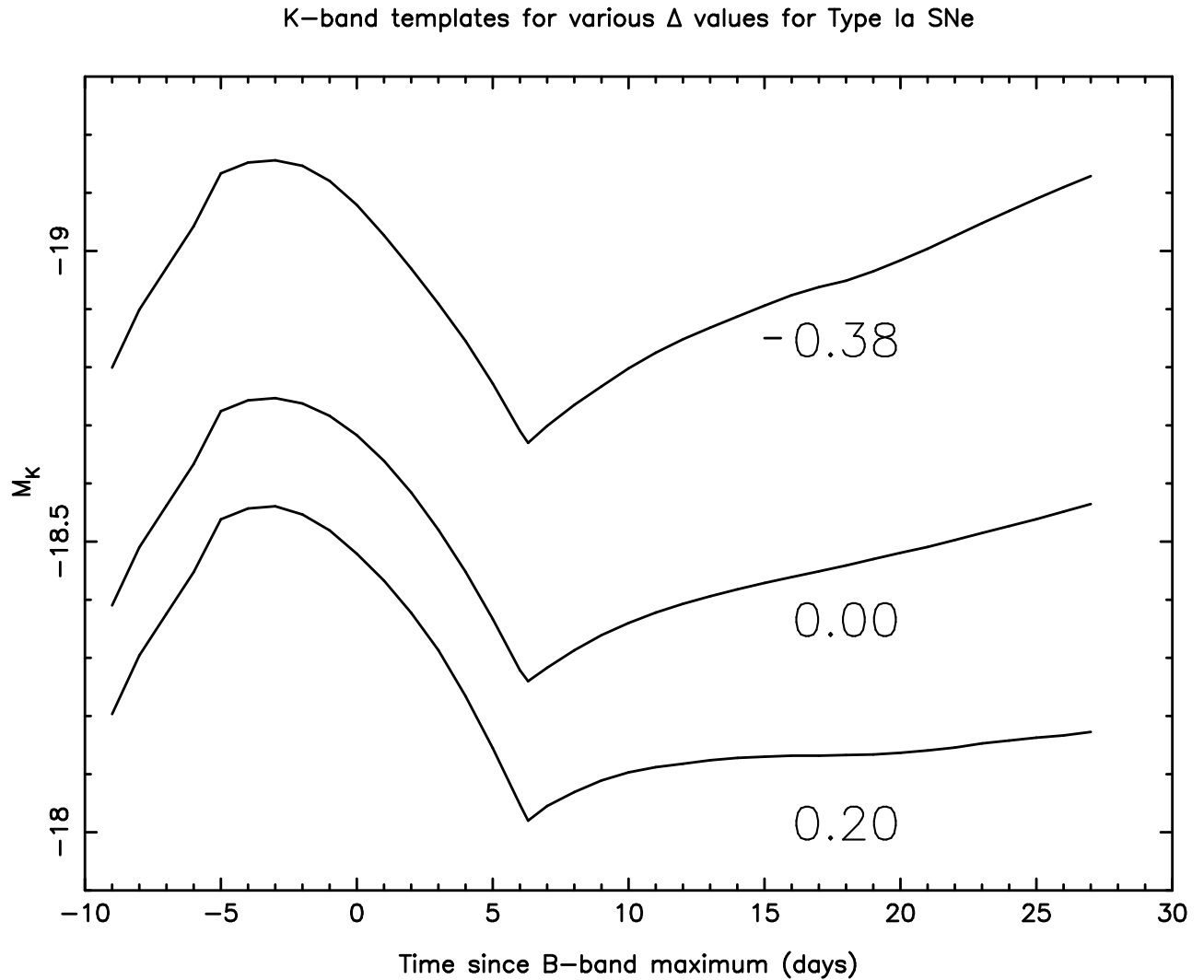


Fig. 12.— Since $K = V - (V-K)$, the existence of V-band light curve templates and the $V-K$ relationship from Fig. 9 predict the K-band templates given here.

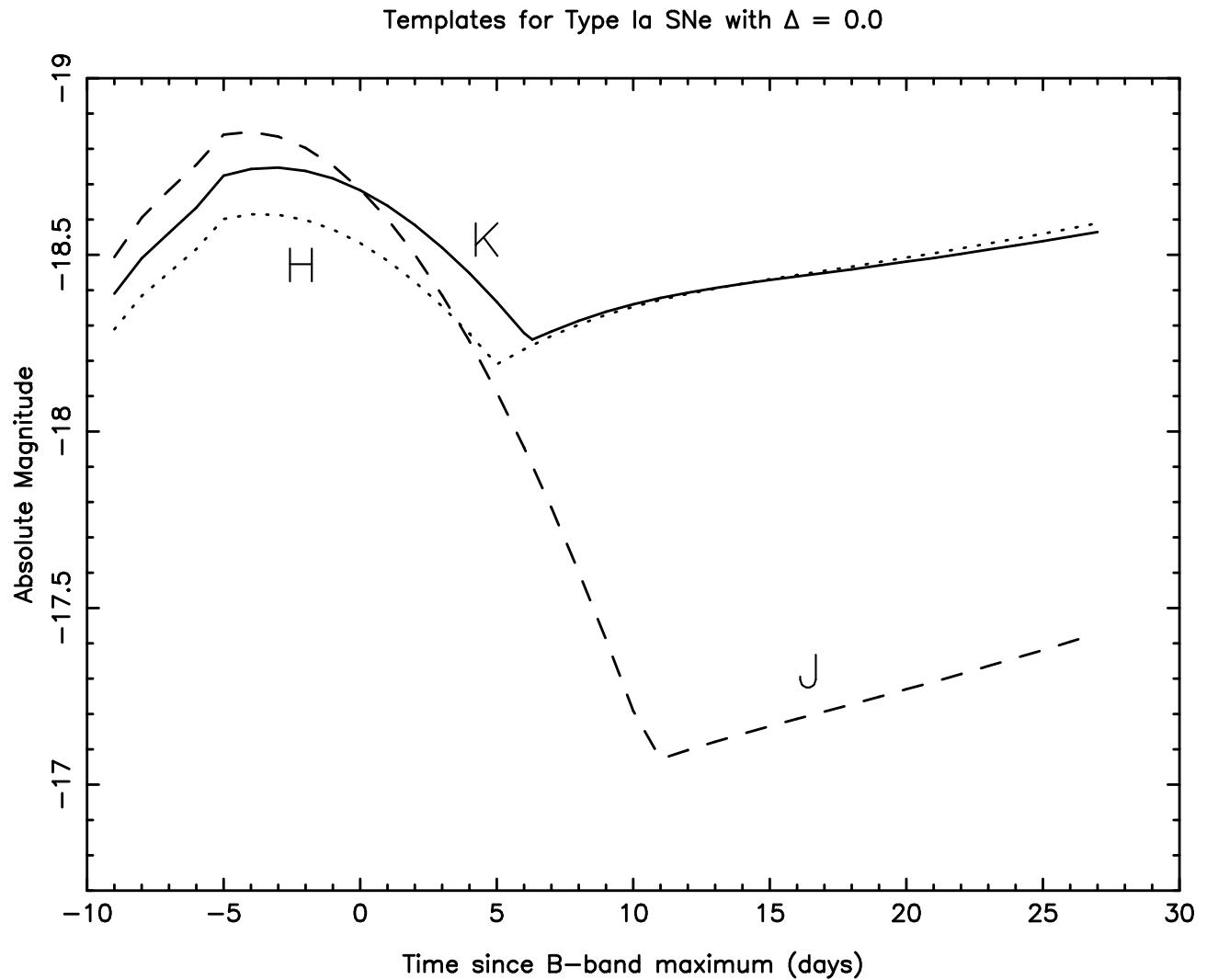


Fig. 13.— Near infrared light curve templates for Type Ia SNe with $\Delta = 0$. J = dashed line; H = dotted line; K = solid line.